

## Double controller of wind induced bending oscillations in telecom towers

Ronaldo C. Battista<sup>1</sup>, Michèle S. Pfeil<sup>1</sup>, Eliane M.L. Carvalho<sup>2</sup> and Wendell D. Varela<sup>\*3</sup>

<sup>1</sup>COPPE Institute, Federal University of Rio de Janeiro, C. Postal 68506, CEP 21941-972, Rio de Janeiro/RJ, Brazil

<sup>2</sup>Department of Civil Engineering, Fluminense Federal University, Passos da Pátria 156-D, São Domingos, CEP 24210-240, Niterói/RJ, Brazil

<sup>3</sup>Department of Structures, Federal University of Rio de Janeiro, Pedro Calmon 550-318, Cidade Universitária, CEP 21941-901, Rio de Janeiro/RJ, Brazil

(Received December 16, 2016, Revised December 7, 2017, Accepted December 9, 2017)

**Abstract.** Wind induced large bending oscillation amplitudes in tall and slender telecommunication steel towers may lead to precocious fatigue cracks and consequent risk of collapse of these structures, many of them installed in rural areas alongside highways and in highly populated urban areas. Varying stress amplitudes at hot spots may be attenuated by means of passive control mechanical devices installed in the tower. This paper gives an account of both mathematical-numerical model and the technique applied to design and evaluate the performance of a double controller installed in existing towers which is composed by a nonlinear pendulum and a novel type of passive controller described herein as a planar motion disk mounted on shear springs. Results of experimental measurements carried out on two slender tubular steel towers under wind action demonstrate the efficiency of the double controllers in attenuating the towers bending oscillation amplitudes and consequent stress amplitudes extending the towers fatigue life.

**Keywords:** vibration control; steel towers; wind induced oscillations; field measurements; passive devices

### 1. Introduction

Large wind induced oscillations of slender telecommunication steel towers may lead to precocious fatigue cracks in welded connections, particularly at the base of very slender tubular structures with thin-walled circular cross sections welded to a thick flange plate. Fatigue cracks propagation may lead to collapse of these structures, which when installed in urban areas may cause severe damage in neighboring properties and even worse physical injuries to the inhabitants. To avoid any of these undesirable events the wind induced oscillation amplitudes – and consequent high stress variations in hot spots of the welded connections – may be attenuated by means of a passive control system installed at the top of the tower.

A number of published works have reported on different passive, semi-active and active auxiliary control systems installed in masts, towers and tall building structures to reduce wind induced oscillations. Breccolotti *et al.* (2007) tested the application of an active mass damper to a full-scale mast; they observed a substantial reduction of the structural resonant response to wind loading and recognized the effects of different types of imperfections of the physical system not simulated in the numerical model such as for example the limitation of available power and computation time delays. A hybrid liquid column controller was conceived and successfully applied to a tall and slender

building model (Battista *et al.* 2008). The use of an adaptive-length pendulum (ALP) damper in which the length of the pendulum is adjusted in real time using a shape memory alloy (SMA) actuator was developed and experimentally verified by Pasala and Nagarajaiah (2014).

It is worth observing that passive control is a prevalent strategy due to its independence from reliance on extra energy input. Impact dampers, characterized by a moving mass between walls, have been used to this end; examples of these are chain impact dampers (Koss and Melbourne 1995), particle dampers (Bryce *et al.* 2000, Lu *et al.* 2010, Lu *et al.* 2016) and liquid impact sloshing dampers (Ueda *et al.* 1992). Other types of passive control systems have also been used, as for example mass-spring-damper devices tuned to the frequencies of a mechanical structural system, best known as tuned mass dampers (TMD), firstly conceived by Frahm (1911) and lately mathematically developed by Den Hartog (1947). These devices were addressed to civil engineering structures by Yao (1972) and since then applied in many successful cases of dynamic control of structural systems. Another passive control system was proposed by Chung *et al.* (2012) which was called friction pendulum tuned mass damper (FPTMD). In this device the restoring and friction forces are provided by the spherical surface of the FPTMD, therefore physical springs and dampers are not needed. Moreover, suspension is not necessary and the installation space is greatly reduced.

Herein passive control devices are more appropriately called tuned dynamic attenuators (TDA). Among the TDA type of passive controllers, the nonlinear pendulum is particularly appropriate to attenuate amplitudes of the low

---

\*Corresponding author, Professor  
E-mail: [wendell@fau.ufrj.br](mailto:wendell@fau.ufrj.br)

frequency fundamental bending vibration mode of tubular structures of circular cross section like chimneys, smoke stacks and telecom towers (Ueda *et al.* 1992, Korenev and Reznikov 1993, Battista 2004, Fallahpasand *et al.* 2015). Conversely, a pendular controller is not appropriate for the second and higher frequency bending vibration modes of tall and slender tower structures. For tubular towers a more appropriate control device to attenuate, for example, vibrations in the second bending mode is achieved by installing at the top of the tower a novel type of passive controller given by a heavy disk mounted on three shear springs which sways in planar motion.

To properly design a mechanical control device some important tasks have to be performed in advance. The number, sequence and extent of these tasks will depend on two main and distinct aspects of the problem scenario: the tower is an existing structure or instead it is being designed. For the existing structure the first needed task is to perform the monitoring of the tower structure under wind action, to be carried out in order to observe and investigate dynamic responses of the tower to random wind forces. Forced mechanical excitation of the tower under almost no wind or under weak wind action (breeze) is a necessary task to easily identify its main vibration characteristics (vibration modes and associated frequencies and modal damping factors). The third needed task is to construct a mathematical-numerical model calibrated (both in frequencies and response amplitudes) with the resulting experimental measurements. Modeling the dynamic interaction between the structural system and the air flow has to take into account, besides the soil-foundation-structure interaction, the proper mathematical description of the wind forces on a slender and flexible tower structure which may have several appendages along its height. In this latter case wind tunnel tests on section model with appendages are recommended to determine the aerodynamic coefficients to feed up the wind forces mathematical model.

The experimentally calibrated mathematical-numerical model will then serve to evaluate the effectiveness of control devices in improving the dynamic behavior and consequent fatigue life of an existing tower. The model may also be used to better design new similar controlled tower structures.

The present paper reports on past case examples of 40m high telecommunication tubular towers under turbulent wind action of low mean velocity which displayed significant amplitudes of oscillation (Battista 2004). Strain measurements at several hot spots around the circular base welded connection of one of these towers (Tower 1), were used to estimate its fatigue life by means of the Palgren-Miner rule (Battista *et al.* 2007). The obtained results raised much concern about the risk of fracture initiation in welded connections and consequent crack propagation leading to collapse on to neighboring urban constructions. A passive control system was then designed and installed in a dozen typical 40 m and 30 m high slender towers. Two of these (Towers 2 and 3) were monitored under wind action to demonstrate the efficiency of the TDA devices in attenuating the towers' oscillation amplitudes and extending

their fatigue life (Battista and Pfeil 2009). It is worthwhile observing that these particular case examples are herein for the first time fully reported, as they were kept for a long time under a clause of secrecy of a contract work.

The mathematical-numerical models and the techniques which were applied in the performance evaluation of the passive control devices are presented herein together with the most relevant results of the experimental measurements carried on these towers; the theoretical model and some experimental results are briefly described in a previous article (Battista and Pfeil 2009). The obtained measurements served to demonstrate the great efficiency of the TDAs.

The usefulness of the previously applied theoretical models of both the structural system and the aerodynamic loading as practical design tools is also demonstrated through the favorable correlation of the theoretical and experimental results.

## 2. Short description of the steel tower structure

The typical 40 meters high slender tubular steel tower structure is illustrated in Figs. 1(a)-1(c). It is composed by eight 5 meters long thin-walled cylindrical modules of circular cross-section. The geometric characteristics of these cylindrical modules fabricated of seam-welded thin steel plates are given in Table 1. Towers 1 and 2 as referred in the present paper are 40 meters high while Tower 3 is composed by modules 3 to 8 (see Table 1) resulting in a 30m high tower.

The typical tower is mounted and aligned by interconnecting the modules' annular flanges by means of high-strength leveling screws and bolts. The bolted annular flanges of two consecutive modules are not in direct contact but are kept clear apart by means of pairs of nuts as shown in the detail of Fig. 1(a). The annular flange of the upper module encircles the outer surface of the tube wall while the flange of the lower module is inserted in the tube (see Table 1 for flange thickness). The two exceptions to this detail are the usual flange connection between modules M7 and M8 with the same diameter and the connection between the base module and the foundation. The base module M1 has at its bottom end a thick annular flange fixed to a massive reinforced concrete (RC) footing through high-strength bolts firmly anchored in the reinforced concrete block (see section AA in Fig. 1). Leveling of the tower bottom flange is done with the aid of 24 bolts.

At the top of the tower there is a circular platform where telecom antennas are fixed. The conductor cables are attached to a rack which is fixed along the tower height adjacent to a maintenance ladder (see section BB in Fig. 1(a)).

## 3. Short description of the double dynamic controllers

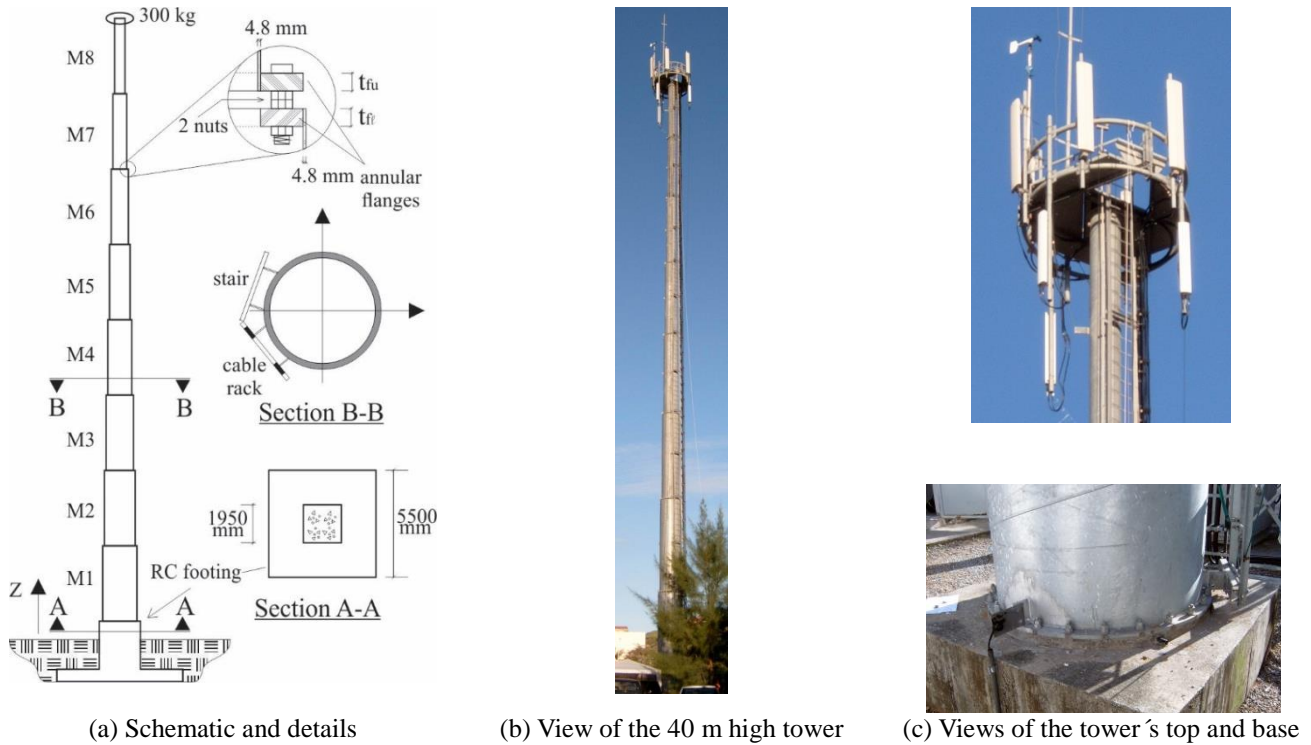


Fig. 1 Typical 40 meters high telecommunication tower

Table 1 Geometric characteristics of the circular cylindrical modules

Modules	Level $z$ (m)	Diameter $D_{ext}$ (mm)	Wall thickness (mm)	Bottom flange thickness (mm)	Top flange thickness (mm)
M1	0 – 5	1286	4.8	25.4	25.4
M2	5 – 10	1138	4.8	25.4	25.4
M3	10 – 15	990	4.8	25.4	25.4
M4	15 – 20	842	4.8	25.4	25.4
M5	20 – 25	728	4.8	25.4	25.4
M6	25 – 30	614	4.8	25.4	25.4
M7	30 – 35	500	4.8	25.4	19.0
M8	35 – 40	500	4.8	19.0	–

Note: Steel ASTM A36

The passive control system designed to attenuate the wind induced vibration of the tower is composed of two mechanical devices installed at its top (see Figs. 2-4): a spatial non-linear pendulum NLP placed inside the top cylindrical module and a tuned dynamic attenuator TDA (i.e a frequency tuned mass-spring-damper device) fixed on the deck floor. The nonlinear pendulum whose parts and mechanical motion are described in detail in Figs. 3 was designed to attenuate amplitudes of the tip of the tower vibrating in its first spatial bending mode. It was designed to keep the amplitudes of the elliptical trajectories of the pendulum mass smaller than the inner radius of the top cylindrical module of the tower while this is set in motion by aerodynamic forces generated by smooth and turbulent wind flow. A rubber Oring (see Fig. 3(b)) was installed

close to the bottom of the solid steel cylindrical pendulum mass in order to smooth the eventual impacts on the tower wall caused by events of strong winds. The threaded sleeve (see Fig. 3(b)) is placed for rod length adjustment in order to reach the desired frequency of the NLP.

The TDA was designed to reduce amplitudes of the tip of the tower vibrating in its second spatial bending mode.

The TDA parts and mechanical motion are illustrated in detail in Figs. 4. It is worth noticing that the coil spring shear stiffness allows the planar motion of the steel disks (mass of TDA) in elliptical trajectories induced by the second bending mode. No torsion mode is excited by wind forces. The tuning of the TDA was performed by adding small pieces of thin steel circular plates and/or adjusting the length of the helical springs. The damping of the TDA is provided by the mechanical damping of the system itself.

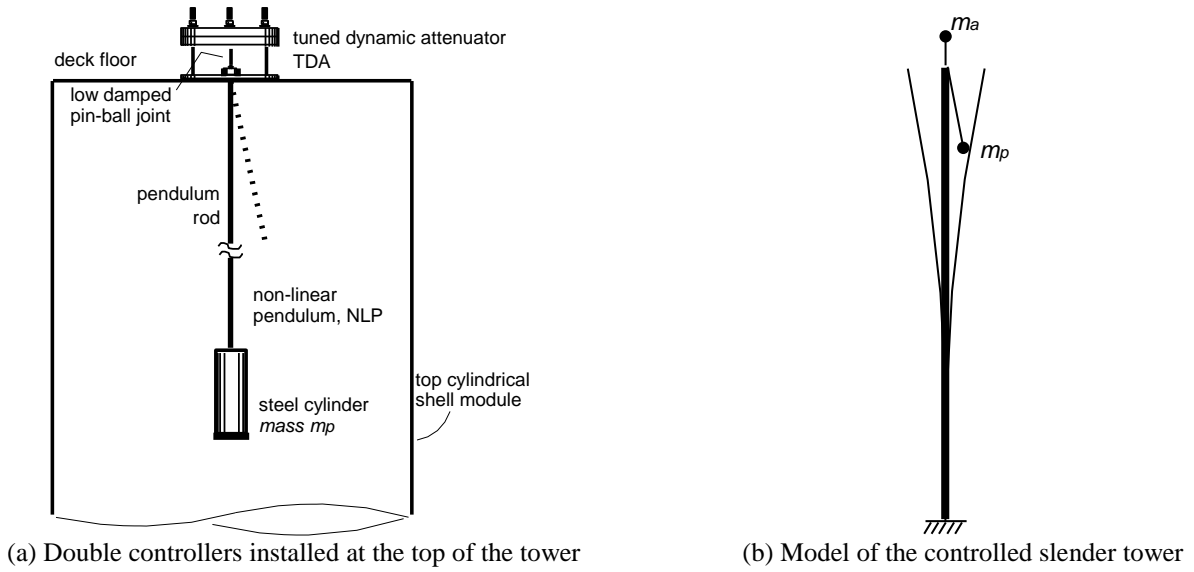


Fig. 2 Schematics of the tower with double controllers

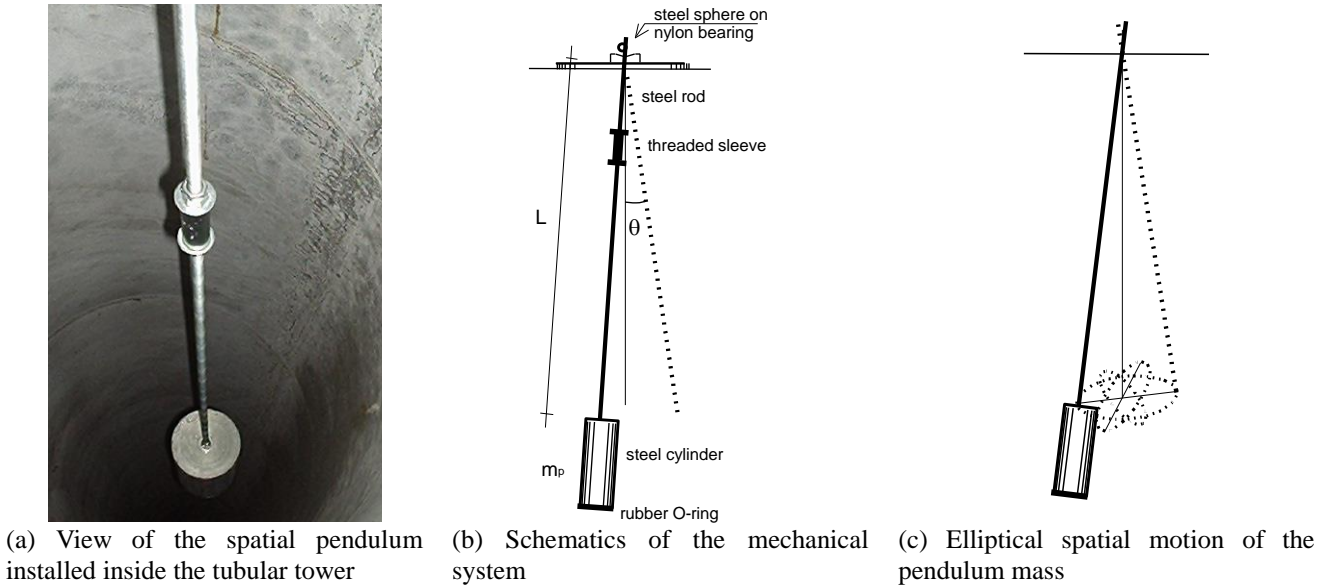


Fig. 3 Details of the NLP controller

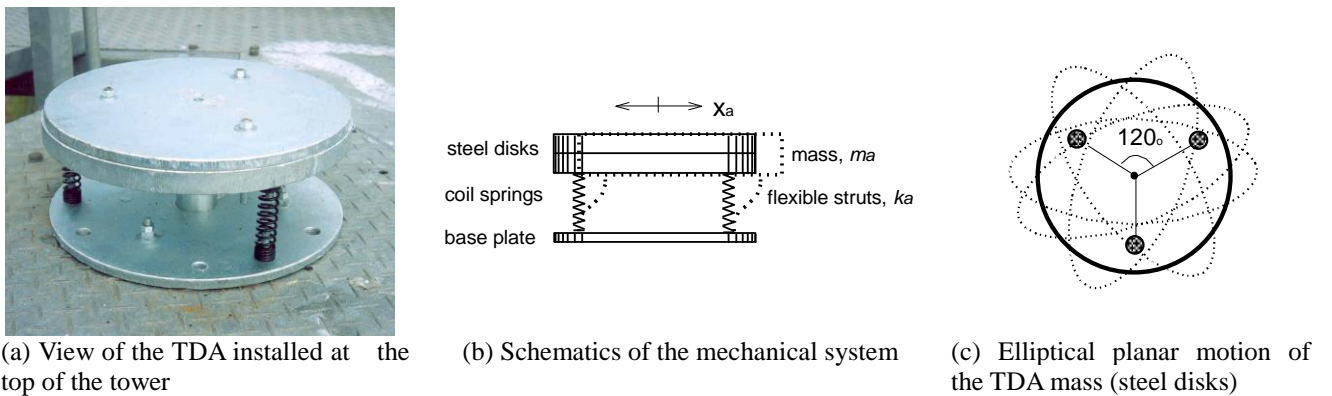


Fig. 4 Details of TDA controller

It should be made clear that the slender tubular steel towers were designed to resist these rare strong wind forces and the role played by the controllers is to reduce top tower displacements and consequent stresses in welded connections, and in this way to enhance the fatigue life of the tower structure under ordinary and frequent wind action.

It should be pointed out that passive control mechanical devices conceived to attenuate wind induced lateral bending amplitudes of a tall and slender tubular tower of varying circular cross-section diameter along its height may be designed on the basis only of the modal dynamic properties of the structural system that are independent of the wind flow characteristics and temperature variations. For moderate wind velocities motion-induced (aeroelastic) wind forces are negligible and hence no modal parameters variations are expected. Similarly, daily and seasonal temperature variations at the towers locations are too small to change the support and connection conditions and stiffness properties so as to significantly affect frequency and damping values. Therefore no detuning due to modal parameter variation will occur.

Aerodynamic response of these structures is mostly dominated by the first two bending vibration modes which in general have well-spaced frequency values. Modal damping factors may be dependent on the soil foundation interaction, particularly in the case of direct foundations in cohesive soil stratum.

Having well-spaced frequency values the dynamic control for this type of tower structure can be conceived and designed separately for each one of the two dominant vibration modes as there is not any modal coupling during the aerodynamic response of the tower structure under action of smooth or turbulent wind flow. These double controllers were installed in a dozen of existing slender tubular towers and are performing well for the last ten years.

#### 4. Wind measurement and dynamic monitoring of the uncontrolled tower

Monitoring of the 40 m high steel Tower 1 was carried out (Battista 2004) to observe and investigate its dynamic response and overall behavior under the low average velocity of frequent regional winds. The structure was instrumented with several sensors, as illustrated in Figs. 5. Accelerometers ( $\sim 0\text{-}1$  g and  $\sim 0\text{-}2$  g,  $\sim 0\text{-}50$  Hz, Kyowa, Japan) were installed at the tower's top (see Fig. 5(b)) to pick up the oscillation amplitudes. For the modal identification tests two more accelerometers ( $\sim 0\text{-}1$  g,  $\sim 0\text{-}50$  Hz, Kyowa, Japan) were installed in orthogonal directions at two-thirds of the height of the tower and two others accelerometers ( $\sim 0\text{-}1$  g,  $\sim 0\text{-}50$  Hz, Kyowa, Japan) were installed in orthogonal directions on the edges of the concrete foundation block to pick up its small rocking motion amplitudes allowed by the soil-foundation interaction. One wind-monitor (Young, USA) was installed on a 5 meters high pole fixed at the tower's top (see Fig. 5) to register the wind velocity and direction variations. Ten strain-gages (3 and 5 mm gauge, 120  $\Omega$ , Kyowa, Japan)

were installed to monitor the strains (stresses) variations on the hot spots along the fillet welded connection (see detail in Fig. 5(c)) between the cylindrical thin-walled module and the thick annular flange at the tower's bottom. The acquisition frequency in the experimental tests was 300pps.

Owing to the simplicity of the structure and its dynamic characteristics such as low values of damping ratio and well separated frequencies the modal parameters were estimated through the analysis of the time responses of the structure excited by impulsive forces applied by a man in sway motion at the top of the tower under very low wind velocity. Modal frequencies were taken from the frequency spectra of the resulting acceleration time responses from which the corresponding damping ratios were obtained by applying the logarithmic decrement technique to the band pass filtered signals. Because of the non-axisymmetric distribution of the appendages masses slightly different values of frequencies associated to bending mode shapes in two orthogonal directions were found: 0.39 and 0.41 Hz for the first bending mode shape and 1.95 and 2.03 Hz for the second bending mode. The following damping ratios were obtained: 2.8% for the 1<sup>st</sup> mode and 1.1% for the 2<sup>nd</sup> mode.

This relatively high value of damping ratio for the fundamental mode at 0.4 Hz of the slender tubular steel tower may be explained by the interaction between the concrete block foundation and the soil. The smaller damping ratio in the second bending mode at 2.0 Hz seems to indicate that damping for the tower foundation system is proportional to the modal masses properties.

Figs. 6 show the variations of wind direction and velocity in a typical measurement campaign of 10 minutes duration when the wind blew from SE. The mean wind velocity was equal to 34.2 km/h (9.5 m/s) at the measurement height ( $\sim 45$  meters above ground level). The average wind direction shown in time history of Fig. 6(a) is  $+131^\circ$  North, varying in the range  $-35.6^\circ$  to  $39.9^\circ$  with respect to this average direction. This variation in wind direction was used to characterize the velocity fluctuation components in the along-wind and across-wind directions whose turbulence intensities were estimated to be 24% and 16% respectively.

For the tower under wind action Figs. 7(a) and 7(b) show respectively the time response amplitudes in terms of horizontal accelerations in two orthogonal directions picked up by sensors AC1 and AC2 installed at the tower top. The acceleration time histories measured by the two other accelerometers AC3 and AC4 installed in the same directions (see Fig. 3(b)) of AC1 and AC2 were almost the same showing that no torsional mode has been excited. This was already expected from the high value of the torsional mode frequency (8.74 Hz) given by the numerical model free vibration analysis (see section 6).

Figs. 8(a) and 8(b) show the frequency response spectrum associated to these acceleration time responses where it can be noted the two peaks related to the frequencies of the dominant vibration bending modes of the structural system.

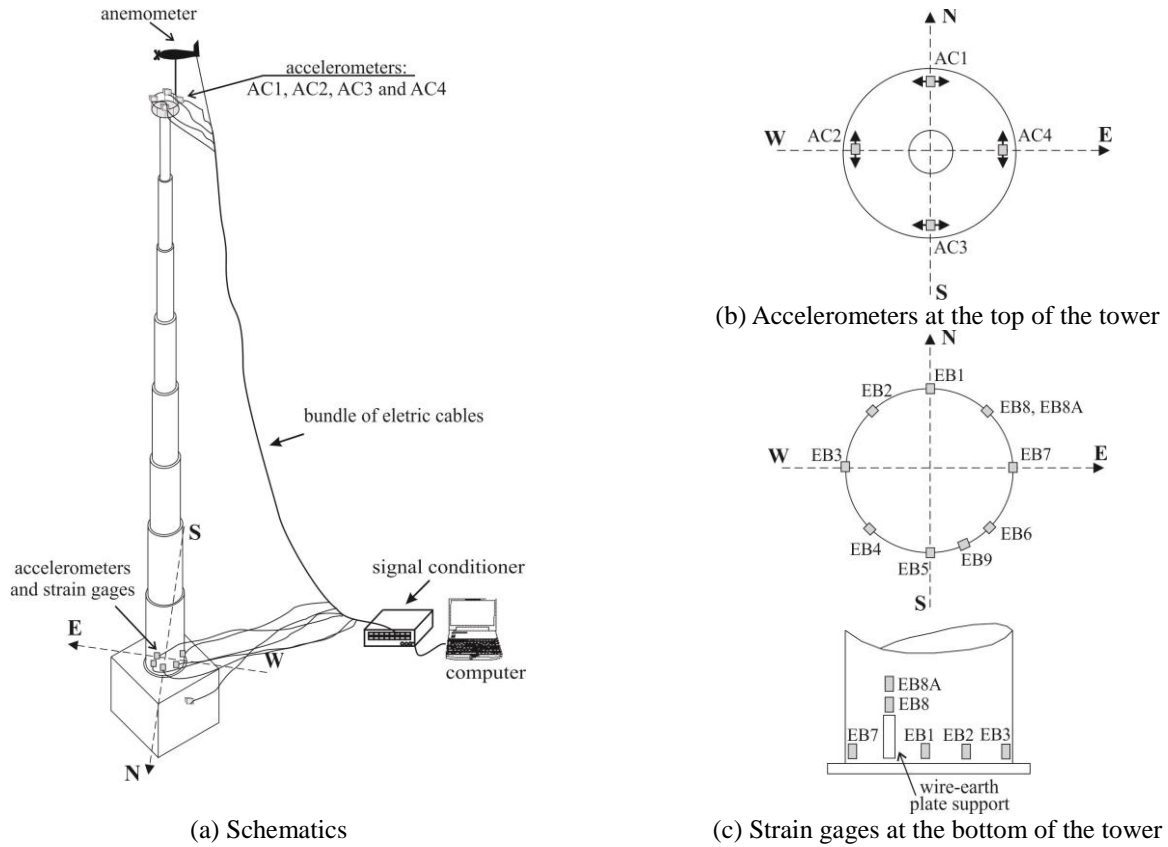


Fig. 5 Instrumentation of the tower structure

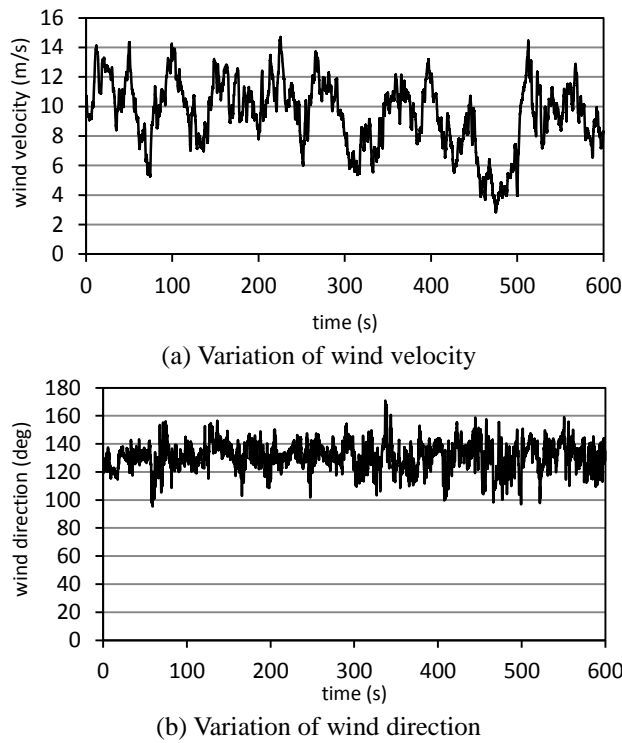


Fig. 6 Experimental measurements of wind velocity in the site of Tower 1

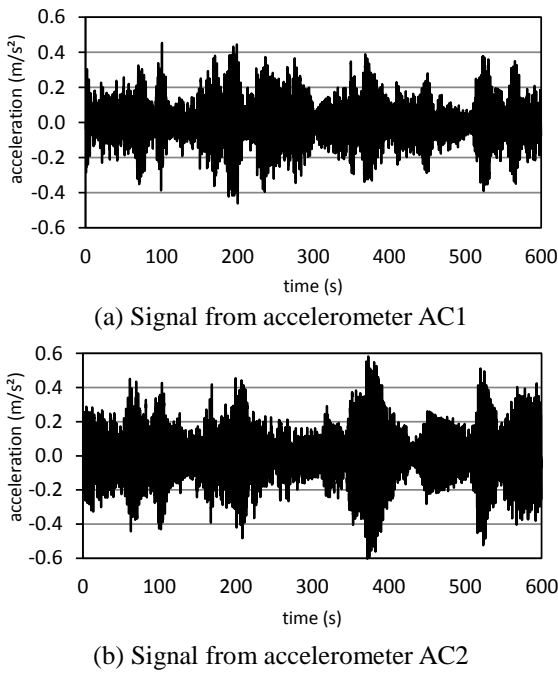


Fig. 7 Horizontal acceleration x time responses measured in two orthogonal directions at the top of Tower 1 (see Fig. 1)

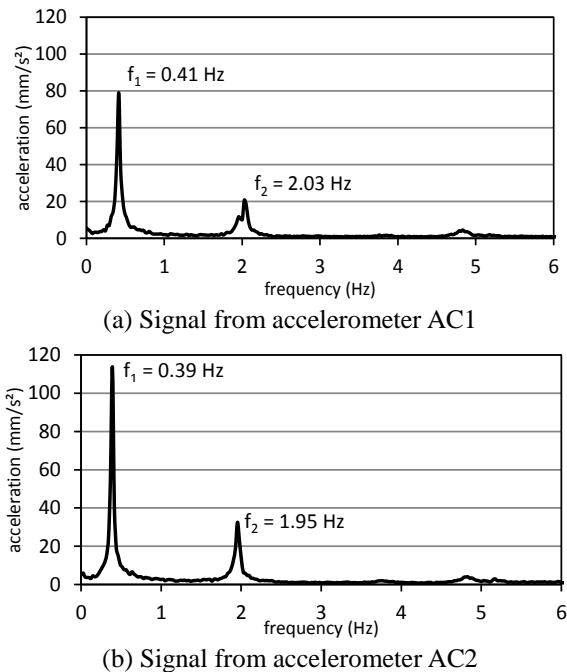


Fig. 8 Frequency response spectra of the acceleration x time responses shown in Figs. 7 (a) and 7(b)

### 5. Mathematical-numerical models

Mathematical-numerical models were specially developed to deal with the focused problem of both original and controlled tower structure under wind action.

The performance of the mechanical control devices was investigated in early design stages by using a combination of the simplified mathematical-numerical models described in what follows.

Although 3D theoretical models were developed for the structure and aerodynamic forces, a planar model of the coupled structure-controllers system was found to be sufficient to demonstrate the performance of the controllers.

This is justified by the observed lack of coupled lateral-torsional motion which allows the responses in along-wind and across-wind directions to be computed separately. The along-wind motion was chosen to perform comparisons between theoretical and experimental results of the uncontrolled structure and between theoretical results of the uncontrolled and controlled structures.

In order to validate the mathematical-numerical model the first analysis was performed considering the uncontrolled structure under wind loading calculated on the basis of the wind velocity measurements displayed in Figs.6. The results in terms of accelerations of the towers top were then compared to the corresponding experimental ones.

#### 5.1 Numerical model of the tower structure

The numerical model of the tower and its foundation consists of 3D frame elements and link elements representing the annular bolted connections between each pair of modules and between the lower module and the reinforced concrete footing (see Fig. 1). The mass moments of inertia of the top deck and the foundation block as well as the mass moments of inertia of the frame elements around the vertical axis are calculated and given as input data. The rotational stiffness (see Table 2) of each of the referred link elements was obtained by applying the so-called component method (CEN 2005). According to this method the overall joint behavior may be assessed by assembling the stiffness characteristics of the individual components (bolts in tension/compression, flange in bending etc) with the aid of mechanical models composed by springs and rigid links. In this case one spring is assigned to each bolt location around the connection circumference. The spring stiffness is obtained by combining the axial stiffness of the bolt and that of an angle section composed by portions of the flange and the module wall according to the model proposed by Faella *et al.* (2000).

The numerical model also considers the footing – soil interaction. This was firstly represented by vertical springs uniformly distributed at the bottom of the square footing.

The stiffness of these springs was obtained by using the volumetric coefficient of vertical subgrade reaction of medium sand soil stratum (Bowles 1997). Then the moments of these vertical spring reactions due to unit rotations of the concrete block around X and Y horizontal axes were calculated and in this manner the soil-structure interaction could be represented by rotational springs in two orthogonal directions whose stiffness are given in Table 2.

Table 2 Rotational stiffness of flange joints

Flange joint between modules	Base/M8	M8/M7	M7/M6	M6/M5	M5/M4	M4/M3	M3/M2	M2/M1
Rotational stiffness (kN.m/rad)	117,000	60,000	46,000	40,000	34,000	29,000	20,000	12,000

## 5.2 Wind forces in the tower structure

### 5.2.1 Wind forces due to turbulent flow

For large-scale turbulence, the instantaneous aerodynamic forces (see Fig. 9(a)) per unit length may be written as follows:

$$F_D(t) = \frac{1}{2} \rho V(z,t)^2 C_D(z) D(z) \quad (1a)$$

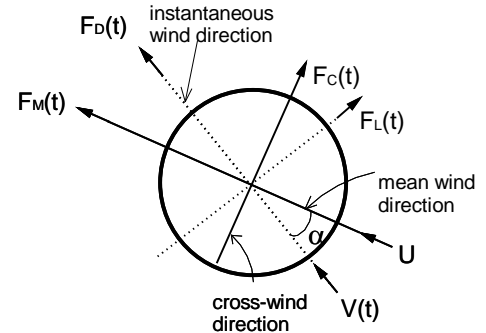
$$F_L(t) = \frac{1}{2} \rho V(z,t)^2 C_{Lm}(z) D(z) \quad (1b)$$

where  $C_D$  and  $C_{Lm}$  are the mean drag and lateral force coefficients,  $D$  is the module diameter,  $V(z,t)$  is the wind velocity and  $\rho$  is the air density. In Eqs. (1(a)) and (1(b)) the aerodynamic damping is being neglected.

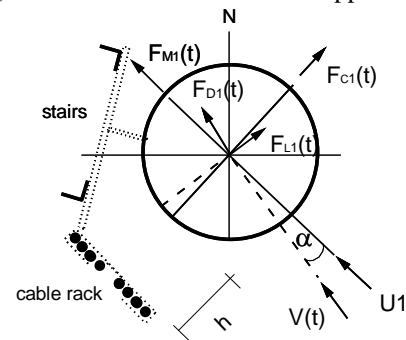
The aerodynamic drag and lateral force coefficients for each wind direction are to be determined by means of experimental wind tunnel tests taking into account the interference effects promoted by the existing appendages. In the absence of data from such tests some justified simplifications were adopted to describe the wind forces bearing in mind that the purpose of the theoretical analysis is to represent the tower's uncontrolled and controlled responses in terms of the amplitudes of the dominant bending modes. With this perspective only the aerodynamic forces on the five upper modules were taken into account. The wind force model is based on the wind velocity ( $V$ ) and direction time histories (Figs. 6) measured 5 m above the tower's top. The variation of the mean wind velocity  $U$  with the height  $z$  above ground is estimated from the power law (Simiu and Scanlan 1996) by considering the exponent value in accordance with the measured turbulence intensity in the along-wind direction at height  $z$  equal to 45 m. On the basis of the estimated value of the integral scale  $L_u^z$  equal to 50 m at the tower top (Counihan 1975), in the present work the fluctuating component of wind velocity is considered in full correlation along the height of the five upper modules.

Considering the location of the ladder in relation to the wind direction  $UI$  and that it is composed of very slender largely spaced bars, its effect on the mean aerodynamic coefficients of the circular cylindrical modules was assumed to be negligible.

The mean drag coefficient of the isolated circular section was calculated according to ESDU (1986) as a function of Reynolds number modified to take into account the turbulence characteristics of the approaching flow and the surface roughness. Table 3 shows the values obtained for  $C_D$  on the basis of the mean wind velocity at mid length of each module considering the measured value  $U(z=45\text{ m})$  equal to 9.5 m/s.



(a) Tower cross-section without appendages



(b) Tower cross-section with appendages

Fig. 9 Directions of wind force components

The variation of the drag coefficient for the circular section due to the presence of the cable rack (likened to the one of a plane plate parallel to the air flow located at a certain distance  $h$  from the cylindrical module wall) was obtained according to Buresti and Lanciotti (1992) as a function of the ratio  $h/D$  and Reynolds number. It is shown in Table 3 that in the present case the variation of  $C_D$  is negligible. Also shown in this table are the resulting mean lateral force coefficients  $C_{Lm}$ .

The drag and lateral forces on the circular cylindrical modules are to be combined with the corresponding forces on the existing appendages (cable rack, antennas etc.) at each time instant. Considering the wind direction and the narrow exposed dimension of the cable rack in comparison to the cylindrical module diameter, negligible drag and lateral forces may be estimated on this component for mean wind direction. The aerodynamic forces on the antennas were also found to be negligible for  $UI$  wind direction. The along-wind and cross-wind force components,  $F_M$  and  $F_C$  (see Fig. 9(a)), are obtained by vector summation of forces  $F_D$  and  $F_L$  at each time instant as a function of the angle  $\alpha$  between the wind velocity vector and the mean wind velocity direction.

### 5.2.2 Wind forces due to vortex-shedding

Table 3 also presents the critical wind velocities  $U_{cr1}$  and  $U_{cr2}$  associated respectively to the first and second vibration

Table 3 Mean aerodynamic coefficients and critical wind velocities related to the upper five modules

Modules	Level $z_m$ (m)	$U$ (m/s)	$Re$	Circular section $C_D$	Circular section and close plate strip		$U_{cr1}$ (m/s)	$U_{cr2}$ (m/s)
					$C_D$	$C_{Lm}$		
M8	37.5	9.2	$3.1 \times 10^5$	0.52	0.51	0.10	1.0	4.9
M7	32.5	9.0	$3.0 \times 10^5$	0.52	0.51	0.10	1.0	4.9
M6	27.5	8.7	$3.5 \times 10^5$	0.51	0.50	0.13	1.2	6.0
M5	22.5	8.3	$4.0 \times 10^5$	0.50	0.50	0.15	1.4	7.1
M4	17.5	7.9	$4.4 \times 10^5$	0.50	0.53	0.17	1.6	8.2

modes calculated for each module diameter on the basis of Strouhal number equal to 0.2. By comparing these critical velocities to the mean wind velocity  $U$  estimated at mid length of each module, it can be noted that there was no resonance between the vortex shedding frequency and that associated to the first vibration mode during the measured event; for the second mode, resonant vortex cells could be formed at modules M4 and M5 though with little influence in bending behavior considering the height of the module above ground and the large turbulence intensity. Hence, understanding that no lock-in condition is feasible to occur for mean wind velocities greater or equal to the measured one, the cross-wind force per unit length on the cylindrical module due to vortex-shedding was considered as a harmonic function with amplitude depending on the fluctuating lateral force coefficient.

### 5.3 Mathematical models for the double dynamic controllers

The 3D spatial motion of the controlled tower structure (with two passive control devices attached to its top as shown in Figs. 2) is governed by two systems of two coupled differential equations, one for each type of the two applied controllers tuned to distinct tower bending frequencies. The mechanical behavior of each spatial controller may be described more easily herein by simple 2D systems of equations without loss of generality.

The second order differential equations that govern the behavior of each one of the two coupled structure-controller systems are given by the following two pairs of Eqs. (2) and (3), in which the used notation is described in Figs. 3 and 4 that illustrate the structural scheme of each of the two controllers. It should be pointed out that the pendulum and the TDA passive control devices work independently of each other and are tuned to the first and second tower bending modes, respectively.

Hence, coupling motions occurs only between each controller and the tower structure and then Eqs. (2) and (3) are not related. Each pair of equations was solved by means of the Runge-Kutta method.

For a simple nonlinear pendulum attached to the top of the tower with length  $L$ , mass  $m_p$  and period tuned to the structure first bending mode period, the controlled tower motion is governed by the following pair of coupled equations

$$M\ddot{x} + m_p\ddot{x} - m_p L \sin \theta \dot{\theta}^2 + m_p L \cos \theta \ddot{\theta} + Kx + C\dot{x} = F \quad (2a)$$

$$m_p \ddot{x} L \cos \theta + m_p L^2 \ddot{\theta} + m_p g L \sin \theta + c_p \dot{\theta} = 0 \quad (2b)$$

where  $\theta, \dot{\theta}, \ddot{\theta}$  are the pendulum angular displacement, velocity and acceleration;  $x, \dot{x}, \ddot{x}$  are the tower generalized horizontal displacement, velocity and acceleration;  $M, C$  and  $K$  are respectively the structural modal properties of mass, damping and stiffness,  $F$  is the generalized wind force and  $g$  is the acceleration of gravity.

For the TDA controller (with mass  $m_a$ , stiffness  $k_a$  and damping  $c_a$ ) attached to the structure and tuned to the second bending mode frequency, the controlled tower motion is governed by the following coupled pair of equations

$$M\ddot{x} + Kx + k_a(x - x_a) + C\dot{x} + c_a(\dot{x} - \dot{x}_a) = F \quad (3a)$$

$$m_a \ddot{x}_a + c_a(\dot{x}_a - \dot{x}) + k_a(x_a - x) = 0 \quad (3b)$$

where  $x_a, \dot{x}_a, \ddot{x}_a$  are the TDA's horizontal displacement, velocity and acceleration.

## 6. Theoretical versus experimental results for the uncontrolled tower

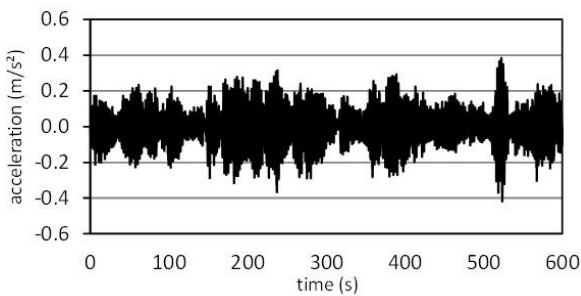
It may be noted in Table 4 the favorable correlation between the theoretical and the experimental natural frequencies of the first three bending modes of the tower. As explained earlier in this paper the experimental values were obtained from man induced vibration tests of the tower under wind of very low velocity (breeze). The pairs of slightly different experimental frequency values given in Table 4 correspond to results obtained for each bending mode in two orthogonal directions (see Fig. 8) while the numerical model yielded only one frequency value for each bending mode. The important role played by the flexibility of the bolted flange connections – and to a minor degree by the soil-footing interaction effect – in the structural behavior may be appreciated by comparing the frequency (0.39 Hz) of the fundamental vibration mode obtained with the refined numerical model to that (0.71 Hz) obtained from

a preliminary model in which the bolted flanges link elements were not included. The soil-footing interaction effect although important in regard to the modal damping ratio had for vibration frequencies a much less important role resulting in only 7% reduction of the fundamental frequency value related to the tower model fixed at its base. No comparison is made for torsional mode as its associated frequency estimated with the numerical model (8.74 Hz) is too high for this mode to be excited by the wind loading.

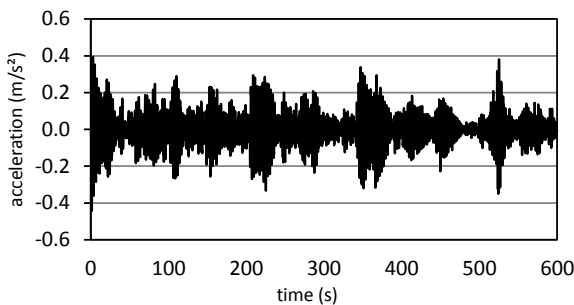
Figs. 10(a) and 10(b) show respectively the along-wind acceleration time responses obtained experimentally and theoretically at the tower top. The responses display a very favorable correlation in both quantitative and qualitative terms, notably the very good correlation in terms of standard deviation ( $0.100 \text{ m/s}^2$  for the experimental and  $0.092 \text{ m/s}^2$  for the theoretical responses). The application of the fast Fourier transform to these time responses yielded the frequency spectra shown in Fig. 11 where a very good correlation between theoretical and experimental results can be observed for both amplitude and vibration frequency of the first bending mode. A favorable correlation between amplitudes may be observed for the second vibration mode, although related to different values of vibration frequency.

Table 4 Theoretical x experimental natural frequencies of the tower structure

Bending Mode	Theoretical frequency (Hz)	Experimental frequency (Hz $\pm$ 0.01 Hz)
1	0.39	0.39 / 0.41
2	1.75	1.95 / 2.03
3	4.15	4.75 / 4.77



(a) Experimental



(b) Theoretical

Fig. 10 Time responses in terms of acceleration in the along-wind direction at the top of the 40 m high Tower 1

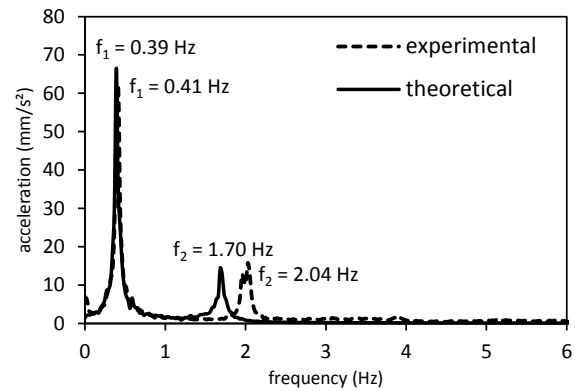


Fig. 11 Experimental x theoretical frequency spectra of the acceleration time responses shown in Fig. 10

The favorable comparison between experimental and theoretical responses amplitudes enables the theoretical model to be used to check the efficiency of the double control system applied to the tower under turbulent wind action.

### 7. Theoretical performance evaluation of the double controller

Table 5 presents the modal properties of the structure and the physical characteristics of the control devices: the nonlinear pendulum and the tuned dynamic attenuator.

Fig. 12 shows the theoretical results obtained with the model described in section 5.3 applied to the along-wind direction. It can be seen that acceleration amplitudes are substantially reduced in both bending modes with the application of the double controller. It can be also seen in the frequency response spectra (Fig. 12) the two pairs of peaks of the controlled response: the first peak in each pair corresponding to the proper controller motion frequency, the second to the controlled structure bending modes frequencies.

Fig. 13 presents the theoretical time response of the pendulum mass in terms of lateral displacements where it can be seen that peak amplitudes are smaller than the inner radius of the tower top module.

Table 5 Characteristics of structure and passive controllers

Modal Characteristics	Structure ( ) <sub>B</sub>	Controller ( ) <sub>A</sub>	Ratios ( ) <sub>A</sub> / ( ) <sub>B</sub>
First bending mode			
Frequency (Hz)	0.390	0.388	0.995
Mass, <i>m</i> (ton)	0.916	0.037	0.040
Damping, $\xi$ (%)	2.8	5.0	1.786
Second bending mode			
Frequency (Hz)	1.750	1.610	0.920
Mass, <i>m</i> (ton)	1.770	0.040	0.023
Damping, $\xi$ (%)	1.1	1.0	0.909

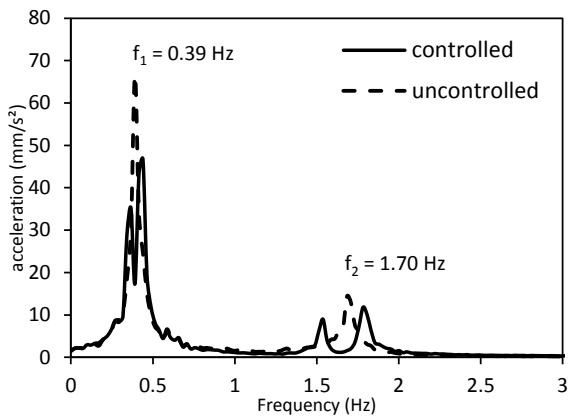


Fig. 12 Theoretical uncontrolled and controlled frequency responses in the along-wind direction at the top of the 40 m high Tower 1

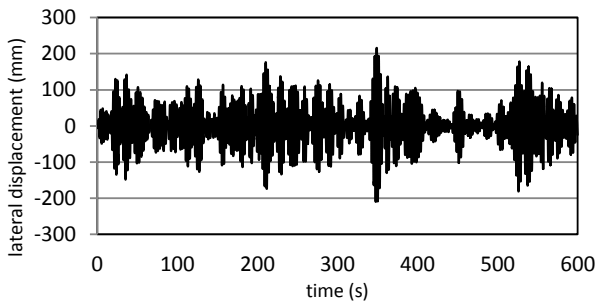


Fig. 13 Theoretical lateral displacement versus time response of the pendulum mass

### 8. Dynamic responses measurements and performance evaluation of the double controller

The 40 m high Tower 2 and 30 m high Tower 3 were equipped with the double controller system and monitored under wind action. The uncontrolled and controlled dynamic responses were obtained by measurements taken in two subsequent 10 minutes time intervals within which negligible deviations on wind mean velocity and on fluctuations spectra were observed. In the first time interval the mechanical control devices were kept locked; in the subsequent time interval they were set free, letting them in full operation.

Fig. 14 shows a comparison between the original uncontrolled and the controlled measured dynamic responses of Tower 2 under a low average wind velocity equal to 2.4 m/s at height  $z$  equal to 45 m and average wind direction  $+120^\circ$  from North.

It can be clearly seen in these frequency response spectra (Fig. 14) that both controllers reduce substantially the amplitudes of the two dominant bending modes at the tower top where they reach maximum values. It can be seen moreover by a direct comparison between the theoretical spectra of Fig. 12 and the experimental spectra of Fig. 14 that the actual performance of both controllers is even better than the expected from the theoretical models.

Fig. 15 shows a comparison between the original uncontrolled and controlled measured dynamic responses of Tower 3. It should be observed that this is a 30 m high tower and therefore exhibits greater natural bending mode frequencies (equal to 0.54 Hz and 2.88 Hz) than the 40m high Towers 1 and 2. During the two 10 minutes time intervals the measurements of the original uncontrolled and the controlled structure were performed, the average wind velocity was equal to 7.1 m/s, the average wind direction was equal to  $+227^\circ$  from North and a 23% along-wind turbulence intensity was estimated; all cited data are related to a point 5m above the tower top.

The successful performance of the mechanical control devices is also illustrated in Fig. 16, where the displacements of the tower's top along North-South direction versus displacements along West – East direction are depicted for both measured uncontrolled and controlled responses of the Tower 3.

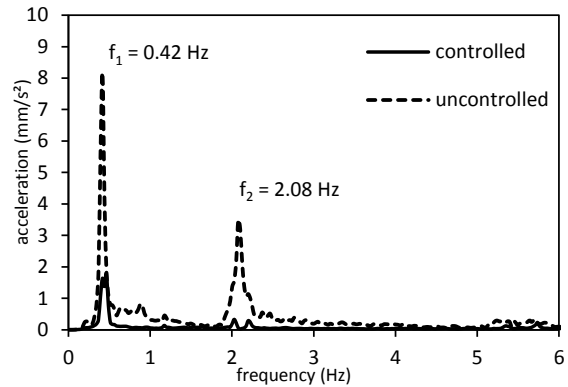


Fig. 14 Frequency spectra of measured uncontrolled and controlled responses in terms of along-wind accelerations at the top of the 40 m high Tower 2

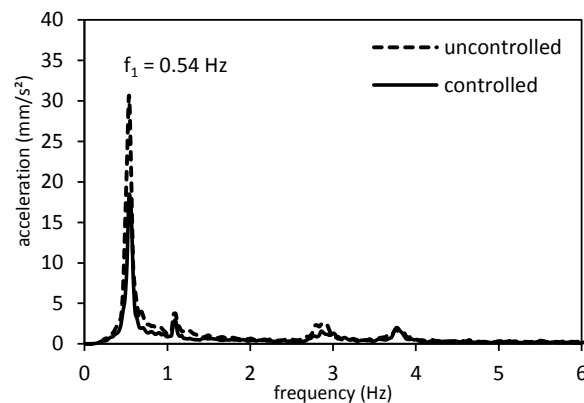


Fig. 15 Frequency spectra of measured uncontrolled and controlled responses in terms of along-wind accelerations at the top of the 30 m high Tower 3

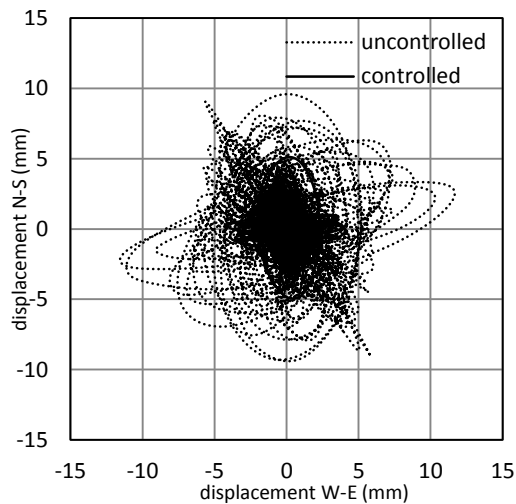


Fig. 16 Measured uncontrolled and controlled motion trajectories of the top of Tower 3

Hence, by reducing oscillation amplitudes consequent reduction of dynamic stresses has greatly extended the fatigue life of these steel tower structures, complying with the main objective of the tailored designed controllers. For example, at the fillet weld connection between the thin wall of the module M1 and the thick flange at the base of the tower (point EB1, Fig. 5(c)) the fatigue life of the uncontrolled structure, equal to 6.7 years (Battista *et al.* 2007), was extended to 29 years by installing the double control system.

## 9. Conclusions

Structural dynamic monitoring of tall and slender telecom steel towers combined with mathematical models for aerodynamic forces and dynamic control were used to design simple and robust double controllers. One a nonlinear pendulum and the other a novel type of passive controller: a planar motion steel disk mounted on shear springs. The pendulum tuned to the first vibration mode of the tower and the planar motion disk tuned to its second vibration mode in order to reduce substantially the amplitudes of the two dominant bending modes.

The successful performance of this control system is herein demonstrated through experimental measurements carried out on two existing towers. It is worthwhile stating that over a dozen of telecom towers fitted with double controllers have had their fatigue life well extended being in successful operation for the last ten years.

This achievement was only possible with the development of mathematical-numerical models of the structural system, which were firstly validated by means of correlations of theoretical frequency and time responses with their experimental counterparts obtained from field measurements of uncontrolled tower structures under wind action.

The structural system tower-foundation was simulated by a refined 3D finite element model, considering the

flexibility of the steel connections between the thin-walled steel circular cylindrical modules that compose the steel towers, as well as the rotational stiffness of the foundation block embedded in the soil.

A relevant conclusion drawn from the theoretical *versus* experimental correlations of aerodynamic responses of typical towers is that the steel connections of the modules played an important role in the vibration modes frequencies, while the foundation-soil interaction effect was of minor importance in all the monitored units.

Dynamic monitoring of some typical towers were by its turn fundamental not only to validate the mathematical-numerical model employed in the design of the mechanical control system but also to carry out structural sensitivity analyses and to a better understanding of the aerodynamic behavior and performance of the controlled structural system.

## Acknowledgments

The research work reported in this paper was financially supported by Conselho Nacional de Desenvolvimento Científico e Tecnológico – CNPq, the Brazilian agency for scientific and technological development. The authors acknowledge the support given by the Brazilian telecom companies, Claro and Vivo through the Agreement for design and commissioning of the dynamic controllers.

## References

- Battista, R.C. (2004), Design and commissioning of mechanical devices to attenuate the wind induced oscillations of telecommunication towers (*in Portuguese*), PEC5211, Fundação Copetec, Rio de Janeiro, Brazil.
- Battista, R.C. and Pfeil, M.S. (2009), “Double controller of wind induced oscillations in telecom towers”, *Proceedings of the International Seminar on Modeling and Identification of Structures Subjected to Dynamic Excitation*, Bento Gonçalves, Brazil, July.
- Battista, R.C., Carvalho, E.M.L and Souza, R.A. (2008), “Hybrid fluid-dynamic control devices to attenuate slender structures oscillations”, *Eng. Struct.*, **30**(12), 3513-3522.
- Battista, R.C., Carvalho, E.M.L, Pfeil, M.S. and Varela W.D. (2007), “Fatigue life estimates for a telecommunication tower under wind action”, (*in Portuguese*), *Revista da Escola de Minas*, **60**(2), 401-408.
- Bowles, J.E. (1997), *Foundation Analysis and Design*, (5th Edition), The McGraw-Hill Companies Inc., New York, NY, USA.
- Breccolotti, M., Gusella, V. and Materazzi A.L. (2007), “Active displacement control of a wind-exposed mast”, *Struct. Control Health Monit.*, **14**(4), 556-575.
- Bryce, L.F, Eric, M.F. and Steven, E.O. (2000), “Effectiveness and predictability of particle damping”, *Proceedings of the SPIE's 7<sup>th</sup> Annual International Symposium on Smart Structures and Materials: Damping and Isolation*, Newport Beach, USA, April.
- Buresti, G. and Lanciotti, A. (1992), “Mean and fluctuating forces on a circular cylinder in cross-flow near a plane surface”, *J. Wind Eng. Ind. Aerod.*, **41**(1-3), 639-650.
- Chung, L.L., Wu, L.Y., Lien, K.H., Chen, H.H. and Huang, H.H. (2012), “Optimal design of friction pendulum tuned mass

- damper with varying friction coefficient”, *Struct. Control Health Monit.*, **20**(4), 544-559.
- Counihan, J. (1975), “Adiabatic atmospheric boundary layers: a review and analysis of data from the period 1880-1972”, *Atmos. Environ.*, **9**(10), 871-905.
- Den Hartog, J.P. (1947), *Mechanical Vibrations*, (3rd Ed.), McGraw Hill Book Company Inc., New York, NY, USA.
- EN 1993-1-1 (2005), Eurocode 3: Design of steel structures - part 1-1: general rules and rules for buildings, Brussels.
- ESDU 80025 (1986), Mean forces, pressures and flow field velocities for circular cylindrical structures: single cylinder with two-dimensional flow, London.
- Faella, C., Piluso, V. and Rizzano, G. (2000), *Structural Steel Semi-Rigid Connections*, CRC Press LLC, Washington DC, USA.
- Fallahpasand, S., Dardel, M., Pashaei, M.H. and Daniali, H.R.M. (2015), “Investigation and optimization of nonlinear pendulum vibration absorber for horizontal vibration suppression of damped system”, *Struct. Des. Tall Spec. Build.*, **24**(14), 873-893.
- Frahm, H. (1911), *Device for Damping Vibrations of Bodies*, US Patent 989958A, USPTO, Alexandria, VA, USA.
- Korenev, B.G. and Reznikov, L.M. (1993), *Dynamic Vibration Absorbers Theory and Technical Applications*, John Wiley & Sons Inc., Chichester, WS, England.
- Koss, L.L. and Melbourne, W.H. (1995), “Chain dampers for control of wind-induced vibration of tower and mast structures”, *Eng. Struct.*, **17**(9), 622-625.
- Lu, Z., Lu, X.L. and Masri, S.F. (2010), “Studies of the performance of particle dampers under dynamic loads”, *J. Sound Vib.*, **329**(26), 5415-5433.
- Lu, Z., Wang, D., Masri, S.F. and Lu, X. (2016), “An experimental study of vibration control of wind-excited high-rise buildings using particle tuned mass dampers”, *Smart Struct. Syst.*, **18**(1), 93-115.
- Pasala, D.T.R. and Nagarajaiah, S. (2014), “Adaptive-length pendulum smart tuned mass damper using shape-memory-alloy wire for tuning period in real time”, *Smart Struct. Syst.*, **13**(2), 203-217.
- Simiu, E. and Scanlan, R.H. (1996), *Wind Effects on Structures: Fundamentals and Applications to Design*, (3rd Ed.), John Wiley & Sons, New York, NY, USA.
- Ueda, T., Nakagaki, R. and Koshida, K. (1992), “Suppression of wind-induced vibration by dynamic dampers in tower-like structures”, *J. Wind Eng. Ind. Aerod.*, **43**(1-3), 1907-1918.
- Yao, J.T.P. (1972), “Concept of structural control”, *J. Struct. Div. - ASCE*, **98**(7), 1567-1574.